



Comprehensive Evaluation of Near-Real-Time Satellite-Based Precipitation: PDIR-Now over Saudi Arabia

Raied Saad Alharbi ^{1,*}, Vu Dao ², Claudia Jimenez Arellano ² and Phu Nguyen ²

¹ Department of Civil Engineering, College of Engineering, King Saud University, P.O. Box 800, Riyadh 11421, Saudi Arabia

² Center for Hydrometeorology and Remote Sensing (CHRS), Department of Civil and Environmental Engineering, University of California, Irvine, CA 90095, USA; vndao1@uci.edu (V.D.); claudij@uci.edu (C.J.A.); ndphu@uci.edu (P.N.)

* Correspondence: rsalharbi@ksu.edu.sa

Abstract: In the past decade, Saudi Arabia has witnessed a surge in flash floods, resulting in significant losses of lives and property. This raises a need for accurate near-real-time precipitation estimates. Satellite products offer precipitation data with high spatial and temporal resolutions. Among these, the Precipitation Estimation from Remotely Sensed Information using Artificial Neural Networks–Dynamic Infrared Rain Rate near-real-time (PDIR-Now) stands out as a novel, global, and long-term resource. In this study, a rigorous comparative analysis was conducted from 2017 to 2022, contrasting PDIR-Now with rain gauge data. This analysis employs six metrics to assess the accuracy of PDIR-Now across various daily rainfall rates and four yearly extreme precipitation indices. The findings reveal that PDIR-Now slightly underestimates light precipitation but significantly underestimates heavy precipitation. Challenges arise in regions characterized by orographic rainfall patterns in the southwestern area of Saudi Arabia, emphasizing the importance of spatial resolution and topographical considerations. While PDIR-Now successfully captures annual maximum 1-day and 5-day precipitation measurements across rain gauge locations, it exhibits limitations in the length of wet and dry spells. This research highlights the potential of PDIR-Now as a valuable tool for precipitation estimation, offering valuable insights for hydrological, climatological, and water resource management studies.

Keywords: PDIR-Now; satellite precipitation products (SPPs); extreme precipitation; Saudi Arabia



Citation: Alharbi, R.S.; Dao, V.; Jimenez Arellano, C.; Nguyen, P. Comprehensive Evaluation of Near-Real-Time Satellite-Based Precipitation: PDIR-Now over Saudi Arabia. *Remote Sens.* **2024**, *16*, 703. <https://doi.org/10.3390/rs16040703>

Academic Editors: Haobo Li, Suelynn Choy, Yuriy Kuleshov, Mayra I. Oyola-Merced and Xiaoming Wang

Received: 13 January 2024
Revised: 14 February 2024
Accepted: 15 February 2024
Published: 17 February 2024



Copyright: © 2024 by the authors. Licensee MDPI, Basel, Switzerland. This article is an open access article distributed under the terms and conditions of the Creative Commons Attribution (CC BY) license (<https://creativecommons.org/licenses/by/4.0/>).

1. Introduction

In the last decade, the Kingdom of Saudi Arabia has faced a high number of flash floods, which resulted in many losses of lives and property. Specifically, more than 13,000 people were impacted by these floods between 1993 and 2013, which occurred approximately nine times throughout that time period, causing an economic loss of over 20 million USD [1]. Due to the increasing frequency of these flood events, it is crucial to characterize and forecast them for the purposes of flood control and warning [2–4]. Furthermore, Saudi Arabia also suffers from severe drought, which can have severe impacts on the water resources of the region [5]. Thus, it is of extreme importance to have access to accurate precipitation estimates.

Even though there are many factors that impact flooding, precipitation is one of the key influencing factors, and the accuracy of the precipitation estimates has a substantial impact on flood predictions and mitigation strategies [4]. Rain gauges effectively and reliably measure precipitation, but a sparse and uneven gauge network's lack of representativeness is a major concern [6–8]. Moreover, a low-density gauge network also makes it difficult to provide accurate rainfall measurements over a large area [9,10].

Over the past three decades, numerous satellite precipitation products (SPPs) have been developed as alternative sources of precipitation estimates [11–13]. These SPPs are

able to provide information about the spatial variability of precipitation, unlike rainfall gauges, and can be available at fine temporal and spatial resolutions. Hydrological and climatological studies benefit substantially from SPPs as they are capable of providing rainfall estimates over areas with few to none monitoring stations [13–15]. Numerous SPPs with high spatial and temporal resolutions have been produced and are available for free online [8,15]. Some SPPs include: the Tropical Rainfall Measuring Mission (TRMM) [16] by the National Aeronautics and Space Administration (NASA), the National Oceanic and Atmospheric Administration's (NOAA) Climate Prediction Center Morphing Technique (CMORPH) [17], the Climate Hazards Group InfraRed Precipitation with Station data (CHIRPS) [18] by the Climate Hazards Center at the University of California (UC) Santa Barbara, Precipitation Estimation from Remotely Sensed Information using Artificial Neural Networks (PERSIANN) [19], PERSIANN-Cloud Classification System (PERSIANN-CCS) [20], and PERSIANN-Climate Data Record (PERSIANN-CDR) [21] all by the Center for Hydrometeorology and Remote Sensing (CHRS) at UC Irvine.

Due to its precise spatial and temporal properties, SPPs have been extensively used to analyze the life cycle of extreme precipitation events [22]. However, due to retrieval procedures, indirect measurements, and numerical model parameters, SPPs have errors and biases [23–25]. As a result, it is vital to analyze and compare the performance of various SPPs before their implementation [26].

The accuracy of SPPs can also be influenced by the complex interplay between topography and precipitation. Mountains and hills can significantly influence precipitation patterns by directing prevailing winds over their slopes, leading to varied precipitation levels in different regions. In the context of southwestern Saudi Arabia, the study by Al-Ahmadi titled "Spatiotemporal variations in rainfall–topographic relationships in southwestern Saudi Arabia" sheds light on the localized dynamics [27]. The research emphasizes the importance of local topographic factors, including topography, altitude, slope, proximity to ridge, and proximity to the Red Sea, in shaping annual and seasonal rainfall. Specifically, the Asir Mountains emerge as key players, with higher altitudes, more mountainous areas, steeper slopes, and areas closer to ridges correlating with increased rainfall. Notably, the concentration of gauge stations along a coastal strip emphasizes the need for more examination of topography's influence on precipitation variations. Despite advancements in precipitation estimation algorithms, the complex terrain in southwestern Saudi Arabia poses challenges in obtaining reliable quantitative precipitation estimation (QPE), given the rapid changes in precipitation characteristics due to orographic enhancement. As we navigate these complexities, continued research and methodological refinements are crucial for a comprehensive understanding of the relationship between topography and precipitation in such complex terrains.

Among the various SPPs available, PDIR-Now [28] is one of the most recently used satellite-based gridded datasets in hydrological models [11,29,30]. It is one of the latest PERSIANN products developed by the Center for Hydrometeorology and Remote Sensing (CHRS) at the University of California, Irvine (UCI). PDIR-Now is a quasi-global near-real-time precipitation product that provides a long record of precipitation estimates, spanning from the year 2000 to the present at a $0.04^\circ \times 0.04^\circ$ spatial resolution. Precipitation is better detected by PDIR-Now than by other near-real-time products by the CHRS because it links brightness temperature and rain rate to remedy errors using climatological data. PDIR-Now's high-frequency infrared image sampling allows it to deliver accurate rainfall estimates quickly after precipitation begins. This algorithm is based on the framework of the PERSIANN-CCS algorithm but uses dynamical shifting of the cloud-top temperature and rainfall rate curves using climatology data [28]. Furthermore, the precipitation threshold was lowered from 273 K to 263 K to improve the detection of warm precipitation.

There has been a limited number of studies analyzing SPPs over Saudi Arabia. Kheimi and Gutub [31] evaluated TRMM 3B42, CMORPH, Global Satellite Mapping of Precipitation Microwave-IR Combined Product (GSMaP-MVK), and PERSIANN against rain gauges. The correlation coefficients (CC) of TRMM 3B42, CMORPH, GSMaP-MVK, and PER-

SIANN were 0.44, 0.44, 0.45, and 0.11, respectively. Furthermore, the mean errors (ME) of TRMM 3B42, CMORPH, GSMaP-MVK, and PERSIANN were 0.26 mm/day, 0.62 mm/day, 0.65 mm/day, and 0.30 mm/day. Their probability of detection (POD) was 0.39, 0.52, 0.53, and 0.24 for TRMM 3B42, CMORPH, GSMaP-MVK, and PERSIANN, respectively. This study concluded that even though all products could detect precipitation accurately, they overestimated the amount of rainfall over the study area. Mahmoud et al. [32] assessed the capability of IMERG Early, IMERG Late, and IMERG Final to capture precipitation over Saudi Arabia using gauge data as the ground truth. The main finding from this study is that all products exhibit increased accuracy, with the exception of some regions in the northern part of the study area. Furthermore, they found that the estimates improved from the Early run to the Final run. Sultana and Nasrollahi [33] evaluated the performance of PERSIANN, PERSIANN-CDR, TRMM-RT, TRMM-3B42, and CMORPH over Saudi Arabia using gauge data as the ground truth. The main conclusion in the study was that PERSIANN-CDR, TRMM-3B42, and CMORPH performed best over the study area. Specifically, PERSIANN-CDR, TRMM-3B42, and CMORPH had PODs of 0.322, 0.424, and 0.654 and CCs of 0.171, 0.42, and 0.471. Helmi and Abdelhamed [34] evaluated CMORPH, PERSIANN-CDR, CHIRPS V2.0, TRMM 3B42 V7, and IMERG V6 against rain gauge data from 2000 to 2012. This study found that all these products performed best at an altitude of 500–700 m in the central and northern parts of the country and that CMORPH performed best in their monthly assessment.

Due to the critical need for accurate near-real-time estimates in flood-prone regions and the product's capacity to accurately depict the spatial variation of precipitation, evaluating this product is crucial. Furthermore, this product has never been evaluated over Saudi Arabia. Thus, the first objective in this study is to evaluate the accuracy of PDIR-Now using Saudi Arabian daily gauge precipitation data. The second objective is to assess the capability of the SPP to identify extreme precipitation events. The results of this study can provide an in-depth understanding of the capabilities of this near-real-time product and can lead to more informed water management decisions.

2. Materials and Methods

2.1. Study Area

Saudi Arabia is located between 15°N and 35°N and 35°E and 57°E, as shown in Figure 1. According to the Köppen climate classification system [35,36], the majority of Saudi Arabia is a hot and arid desert; however, the southwest region of Saudi is considered semi-arid [37,38]. Precipitation is scant and infrequent in most regions of Saudi Arabia, with the wet season occurring from October to April [37,39]. During dry months, hardly any precipitation occurs, with the exception of the southwest area of the country [39,40].

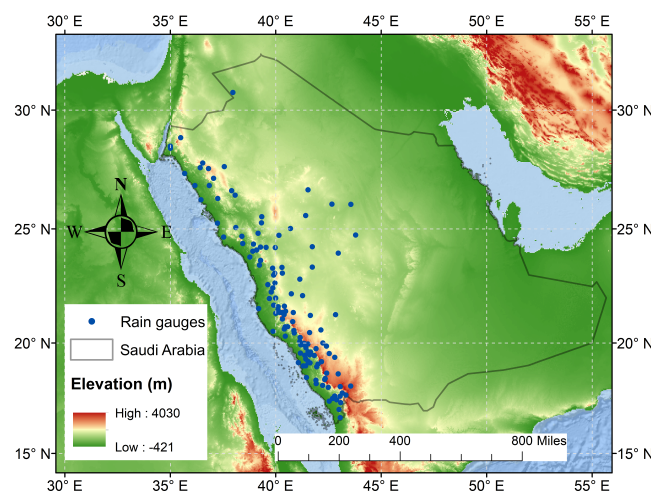


Figure 1. Geographical extent of Saudi Arabia, and distribution of rainfall gauges over the region of study.

2.2. Datasets

2.2.1. Rain Gauges

In this study, the daily rain gauge dataset obtained from the Ministry of Environment, Water, and Agriculture (MEWA) for 130 meteorological observatories across Saudi Arabia (Figure 1) from 2017 to 2022 is used. To ensure the robustness of our analysis, a data quality control process was conducted. This involved an inspection of the dataset to identify and address missing or Not a Number (NaN) values, ensuring consistency throughout the entire study period.

2.2.2. PERSIANN Dynamic Infrared (PDIR-Now)

PDIR-Now is a near-real-time global high-resolution SPP developed by the University of California, Irvine's Center for Hydrometeorology and Remote Sensing (CHRS). The PDIR-Now algorithm considers several factors beyond brightness temperature to estimate precipitation intensity. It utilizes a catalog of cloud types that is created by training self-organizing feature maps (SOFMs) with passive microwave (PMW) data. Then, the rain rate estimation is based on the brightness temperature, size, and texture features of the cloud patches at temperatures below 263 K, utilizing the IMERG PMW precipitation dataset for model training. Furthermore, this algorithm involves the dynamical shifting of cloud-top brightness temperatures–rain rate (Tb-R) curves using rainfall climatology data. The spatiotemporal resolution of 0.04° on a monthly basis is employed to adjust the position of the curves, aiming to correct biases and produce more accurate precipitation estimates. The adjustment is intended to account for regional variations in wetness, generating more precipitation in areas with a wetter climatology and vice versa. Compared to other SPPs, the characteristics of the PDIR-Now algorithm include being a real-time, high-resolution precipitation product with a short delay time (15 min–1 h) [28]. From 2000 forward, PDIR-Now offers quasi-global coverage (60°S–60°N) and high spatiotemporal resolution (almost 0.04° and hourly data) precipitation data. The CHRS database of daily PDIR-Now readings was acquired from the CHRS data portal (<http://chrsdata.eng.uci.edu/> (accessed on 1 December 2023)).

2.3. Methods

Daily satellite precipitation data for each rain gauge were extracted from the nearest grid point in the satellite-based precipitation products, matching the locations of the rain gauges used in this study. The evaluation in this study is divided into two categories: rainfall intensity and extreme rainfall assessments. Statistical metrics were calculated for PDIR-Now using the gauge data as the ground truth. This method is widely adopted for assessing the accuracy of SPPs.

2.3.1. Evaluation Metrics

First, six widely used statistical metrics, shown in Table 1, were applied to assess the accuracy of PDIR-Now across various rainfall rates when compared to the rain gauge observations, with the goal of better understanding the PDIR-Now performance in terms of precipitation amount and occurrence. The correlation coefficient (CC), mean bias (MB), and the root-mean-squared error (RMSE) were used to evaluate the PDIR-Now performance in estimating the amount of rainfall, whereas the probability of detection (POD), the false alarm ratio (FAR), and the critical success index (CSI) were used to evaluate the performance of PDIR-Now in rainfall detection.

Table 1. Statistical metrics employed to gauge the performance of satellite-based precipitation products.

Index	Equation	Optimal Value
CC	$CC = \frac{\sum_{i=1}^n (E_i - \bar{E})(O_i - \bar{O})}{\sqrt{\sum_{i=1}^n (E_i - \bar{E})^2} \sqrt{\sum_{i=1}^n (O_i - \bar{O})^2}}$	1
MB	$MB = \sum_{i=1}^n (E_i - O_i)$	0
RMSE	$RMSE = \sqrt{\frac{1}{n} \sum_{i=1}^n (E_i - O_i)^2}$	0
POD	$POD = \frac{TP}{TP + FN}$	1
FAR	$FAR = \frac{FP}{TP + FP}$	0
CSI	$CSI = \frac{TP}{TP + FP + FN}$	1

Where O_i represents the reference rain gauge data; \bar{O} represents the mean of the reference; E_i represents the PDIR-Now estimation; \bar{E} represents the mean of the estimation; and n refers to the number of samples. In the case of the last three indices, TP represents the number of precipitation events detected within the rain gauges and PDIR-Now synchronously; FN represents the number of precipitation events observed by rain gauges but not PDIR-Now; FP refers to the number of precipitation events detected by PDIR-Now that were not observed by rain gauges. The threshold for defining precipitation occurrence was 0.5 mm/day, as specified by MEWA.

CC quantifies the linear relationship strength between PDIR-Now and the rain gauge variables. MB and RMSE highlight discrepancies between PDIR-Now and the rain gauge measurements, with lower values indicating smaller differences. Additionally, POD assesses PDIR-Now's reliability in detecting precipitation events, FAR measures its tendency to identify unobserved precipitation, and CSI evaluates its proficiency in recognizing precipitation events relative to the rain gauge data. To assess PDIR-Now's capability to detect precipitation, especially intense precipitation, various rain thresholds were used. Table 2 presents the defined rainfall intensity classes within the scope of the study, along with their corresponding daily rainfall thresholds.

Given that the study area encompasses arid and semi-arid regions where rainfall is often minimal or absent, we first calculate the metrics for all precipitation throughout the study period and then categorize rainfall data into four classes, including "No Rain", "Light Rain", "Moderate Rain", and "Heavy Rain". The subjective selection of thresholds is carefully considered after analyzing the distribution of the daily data and reviewing different thresholds and classification standards in similar regions. The "No Rain" category covers instances of no rain and instances where the rainfall rate is equal to or less than 0.5 mm/day, implying negligible rainfall. The "Light Rain" category covers instances where the rainfall rate is between 0.5 and 2 mm/day, implying relatively minimal rainfall. The third category, "Moderate Rain", covers a range of rainfall rates between 2 and 10 mm/day, showing a moderate level of precipitation, and the last category, "Heavy Rain", is determined by rainfall rates exceeding 10 mm/day, representing extreme and impactful rainfall events.

Table 2. Rainfall intensity classes defined in the study with their respective daily rainfall thresholds in mm/day.

Index	Equation
No Rain	Rainfall Rate ≤ 0.5
Light Rain	$0.5 < \text{Rainfall Rate} \leq 2$
Moderate Rain	$2 < \text{Rainfall Rate} \leq 10$
Heavy Rain	Rainfall Rate > 10

2.3.2. Extreme Precipitation Analysis

The second part of the study consisted of calculating four common standard extreme precipitation indices to assess PDIR-Now's performance in capturing extreme precipitation events using gauge data as the baseline. These indices, shown in Table 3, were defined by the World Climate Research Programme (WRCP) and have been used all around the globe [41–43]. The four indices were initially calculated for each year within the 6-year period at each rain gauge, then at each station, the mean of the annual extreme index values was computed. Furthermore, the 130 rain gauge stations were classified into three altitude ranges, specifically: <500 m, 500 m–1000 m, and >1000 m. This was implemented to assess the performance of PDIR-Now in capturing extremes at different elevations.

Table 3. The four extreme indices selected for this study with their respective definitions and units.

Index	Descriptive Name	Definition	Units
RX1day	Maximum 1-day precipitation	Annual maximum 1-day rainfall	mm
RX5day	Maximum 5-day precipitation	Annual maximum consecutive 5-day rainfall	mm
CWD	Consecutive wet days	Annual maximum consecutive rainy days	days
CDD	Consecutive dry days	Annual maximum consecutive dry days	days

3. Results

3.1. Analysis of Rainfall Estimation Errors

The evaluation of PDIR-Now against the gauge data was performed at a daily scale, involving the calculation of several metrics, including the CC, MB, RMSE, POD, FAR, and CSI. To assess the results, the mean of each of the metrics over the study area was calculated for each rainfall category, and the spatial distribution of the metrics was visually assessed. The results reveal a CC of 0.33, a MB of 0.07 mm/day, and a RMSE of 3.04 mm/day (Figure 2). Figure 3 shows the CC, MB, and RMSE results for the three rainfall categories, "Light Rain", "Moderate Rain", and "Heavy Rain". PDIR-Now exhibits the largest mean absolute CC in the "Heavy Rain" category, 0.29, whereas the "Moderate Rain" and "Light Rain" categories had lower mean absolute CCs, 0.17 and 0.16, respectively. This is as expected given that smaller precipitation rates are more susceptible to errors. The lower CC values during moderate rainfall events could be linked to the orographic effects of the prominent mountainous region in Saudi Arabia [27,44]. In arid regions like Saudi Arabia, the interaction between topography and precipitation is a crucial factor influencing the spatial distribution of rainfall [39]. Mountains can act as barriers to moist air masses, leading to orographic lifting on the windward side and subsequently enhancing rainfall in those areas. Conversely, on the leeward side of the mountains, a rain shadow effect may occur, resulting in reduced rainfall. PDIR-Now exhibits the lowest MB in the "Light Rain" category across all areas evaluated, with a mean of 1.14 mm/day. As expected, the MB increases as the rainfall threshold increases, thus, the "Moderate Rain" and "Heavy Rain" categories show larger, but negative, MB values with a mean of −1.76 mm/day and −14.55 mm/day, respectively. The negative sign of the MB results represents that PDIR-Now underestimates precipitation in the two heavier precipitation categories. Similarly, the RMSE values in the "Light Rain" category are the lowest compared to the heavier precipitation categories, with a mean value of 4.45 mm/day. Just as in the case of the MB, the RMSE increases as the precipitation threshold increases, leading the "Moderate Rain" and "Heavy Rain" categories to have increasingly higher values, with means of 6.65 mm/day and 21.88 mm/day, respectively. In the case of the "Light Rain" and "Moderate Rain" categories, the southwest region of the study area along the coast shows higher RMSE values, once again, due to the orographic effect over this mountainous area. Finally, the "Heavy Rain" category does not show one specific area with higher or lower RMSE values than the rest, and instead, these values vary greatly from one gauge to another.

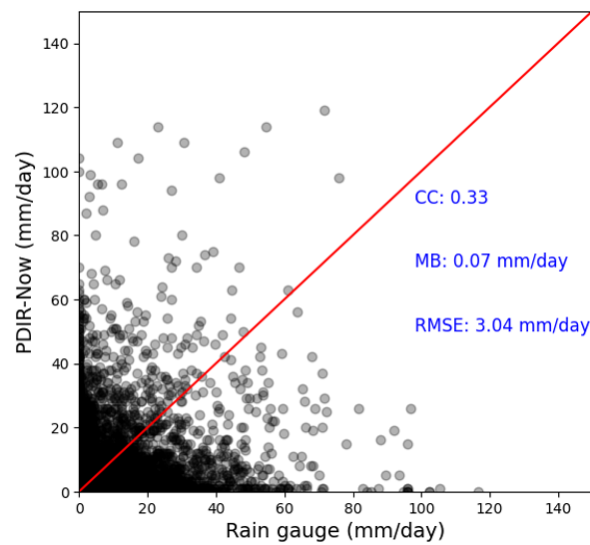


Figure 2. Scatter plot of daily PDIR-Now results compared to the rain gauge observation with statistical indices results. The red line represents the best fit.

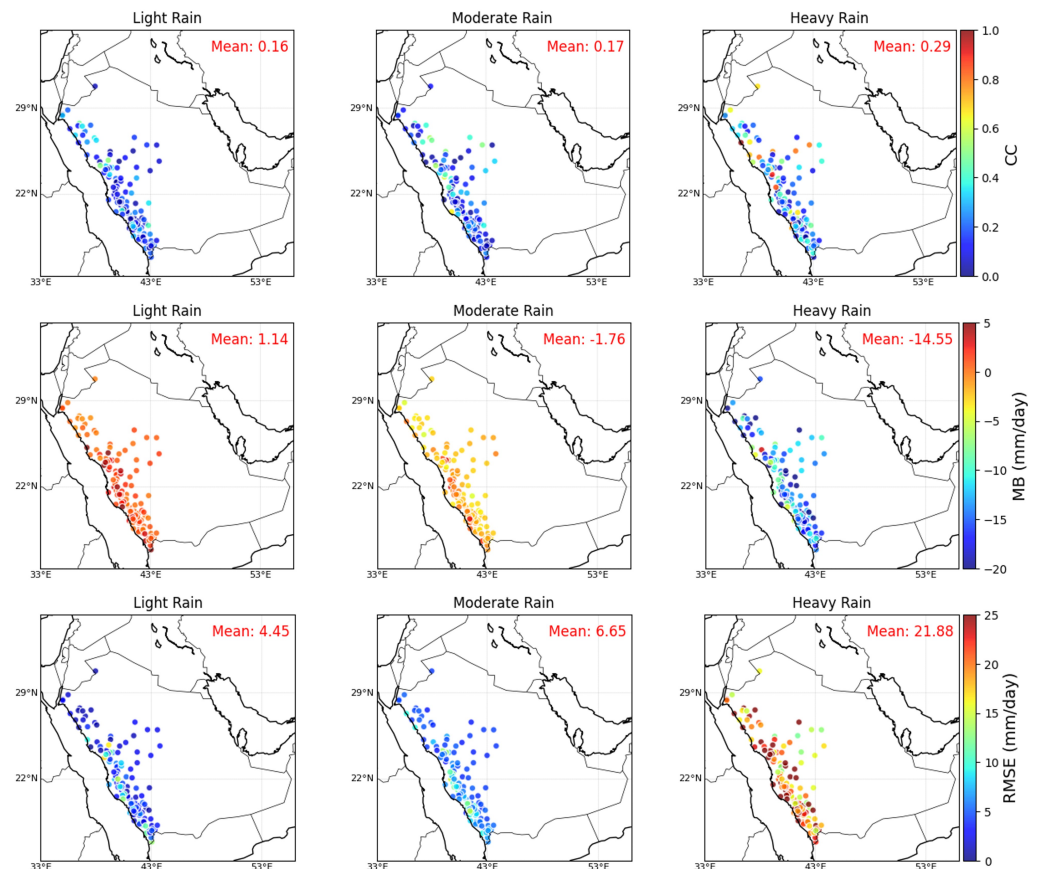


Figure 3. Spatial distribution of CC (upper row), MB (middle row), and RMSE (lower row) of daily PDIR-Now against rain gauge observations for different rain categories with respective mean values.

3.2. Performance Indicator Based on Events

After assessing the results of the rainfall estimation errors, it is necessary to assess the detection capability of PDIR-Now at different rainfall rate thresholds. The result of the rainfall detection in Figure 4 shows that PDIR-Now has a POD of 0.73, a FAR of 0.80, and a CSI of 0.18. While rain gauges along the coast do not achieve high detection performance compared to inland ones, it is evident that the southwestern coast exhibits lower false

alarms (first and second columns). This pattern is reflected in the detection accuracy, as seen in the CSI plot. It is important to note that a threshold of 0.5 mm/day is applied to differentiate between rain and no rain instances for this calculation. More detailed results for rainfall categories such as “Light Rain”, “Moderate Rain”, and “Heavy Rain” are discussed below.

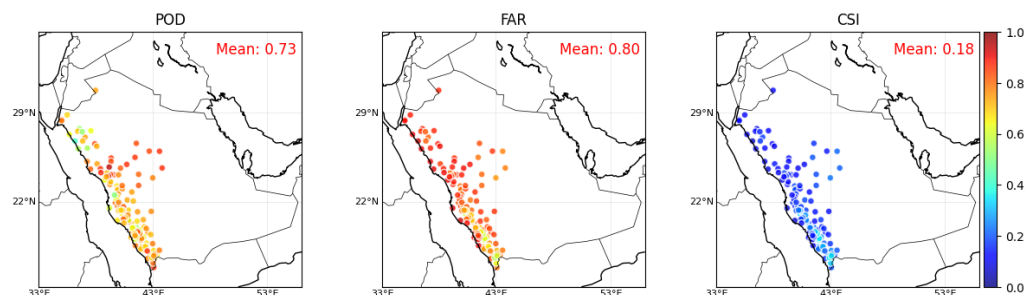


Figure 4. Spatial distribution of POD, FAR, and CSI of daily PDIR-Now against rain gauge observations in rainfall detection.

Figure 5 offers a nuanced insight into the capacity of the PDIR-Now dataset to accurately capture rain events across different rainfall rate categories. The left column of this figure exhibits the great capability of PDIR-Now to capture precipitation in the “Light Rain” category, with mean POD, FAR, and CSI values of 0.47, 0.94, and 0.05, respectively. PDIR-Now performs similarly in all regions of the study area for this category. The POD of PDIR-Now is lower, but FAR decreases with higher rainfall rates, as shown by the middle and right columns of Figure 5. In the case of the “Moderate Rain” category, the POD is substantially lower than in the “Light Rain” category, with a mean value of 0.20. The mean FAR and CSI values obtained were 0.85 and 0.09, respectively. These values indicate that PDIR-Now’s accuracy in detecting moderate precipitation events is higher than in the case of light precipitation detection. Finally, PDIR-Now’s performance slightly increases when detecting heavy precipitation events, as shown in the right column of Figure 5. Despite showing a lower mean POD than in the “Moderate Rain” category, 0.18 specifically, the FAR decreased, and the CSI increased, with values of 0.75 and 0.11, respectively. This indicates that PDIR-Now’s detection of events is slightly lower but more accurate for heavy precipitation events than in the “Moderate Rain” and “Light Rain” categories. The middle and right columns of Figure 5 also reveal that PDIR-Now is more accurate in the middle region of Saudi Arabia than along the coast, as was also depicted by the RMSE previously.

An observation made from the detection results of the rain/ no rain analysis is that the detection is more accurate along the southwestern coast, whereas this is not the case for the different rainfall categories. The discrepancy can be attributed to the more rigorous thresholds set for the categories (Table 2). In this analysis, PDIR-Now is required to meet the criteria for “Light Rain”, “Moderate Rain”, and “Heavy Rain” based on gauge readings, as opposed to a simpler rain/no rain detection.

3.3. Analysis of Rainfall Extremes and Climatic Patterns

The last part of the study was to assess the capability of PDIR-Now at capturing extreme precipitation events. Figure 6 provides a comprehensive overview of several critical climatic and hydrological parameters across all the meteorological stations employed in this study. The top panel shows the results for the mean of the annual maximum daily precipitation amount (RX1day) in mm. The results depict that the RX1day index is similarly captured by PDIR-Now for most of the rainfall gauges, with some minor underestimation. This similitude accompanied by underestimation can be confirmed by the leftmost panel of Figure 7, which shows a high mean CC of 0.50 but a mean bias of -2.83 mm. The mean of the annual maximum five consecutive day precipitation amount, or RX5day index, exhibits similar results, indicating a slight underestimation by PDIR-Now. In regards to the RX5day, the CC and RMSE were 0.53 and -3.10 mm, respectively. The results displayed on the

top panels of Figure 6 and the leftmost panels of Figure 7 indicate that the precipitation distribution of PDIR-Now across gauge locations is in agreement with the precipitation amount captured by the rainfall gauge network.

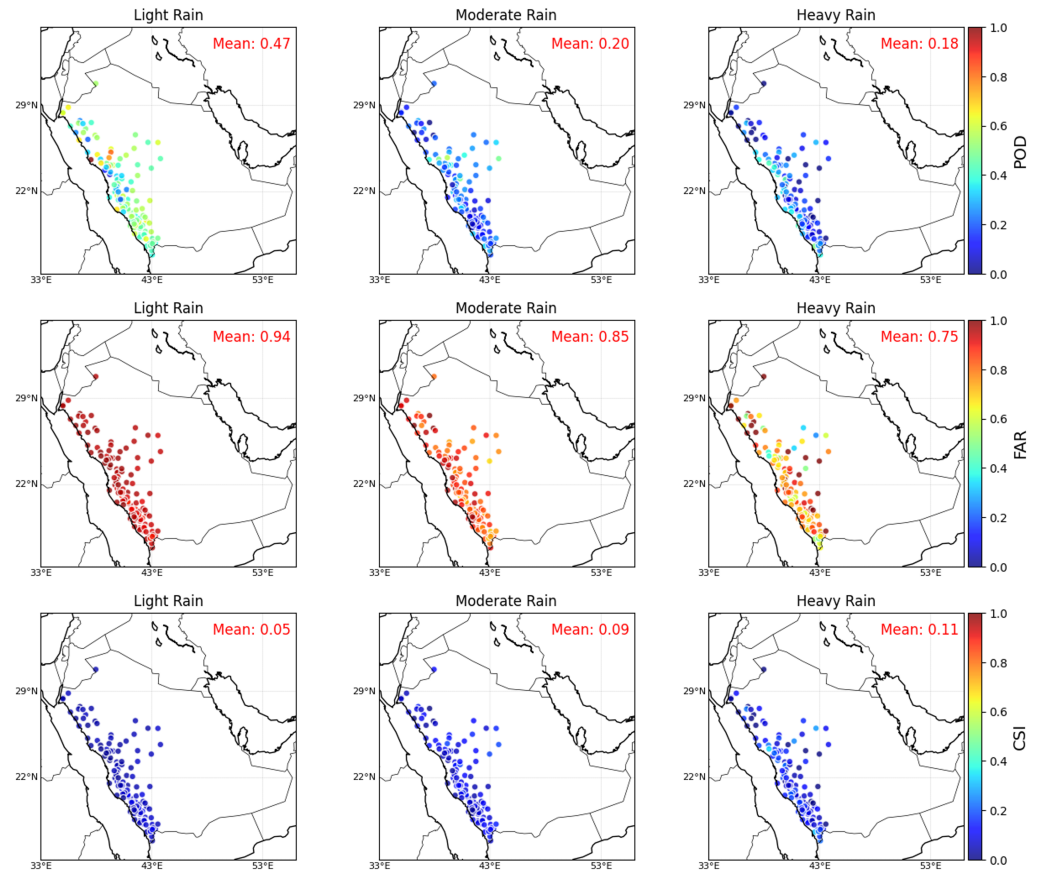


Figure 5. Spatial distribution of POD (upper row), FAR (middle row), and CSI (lower row) of daily PDIR-Now against rain gauge observations for different rain categories with respective mean values.

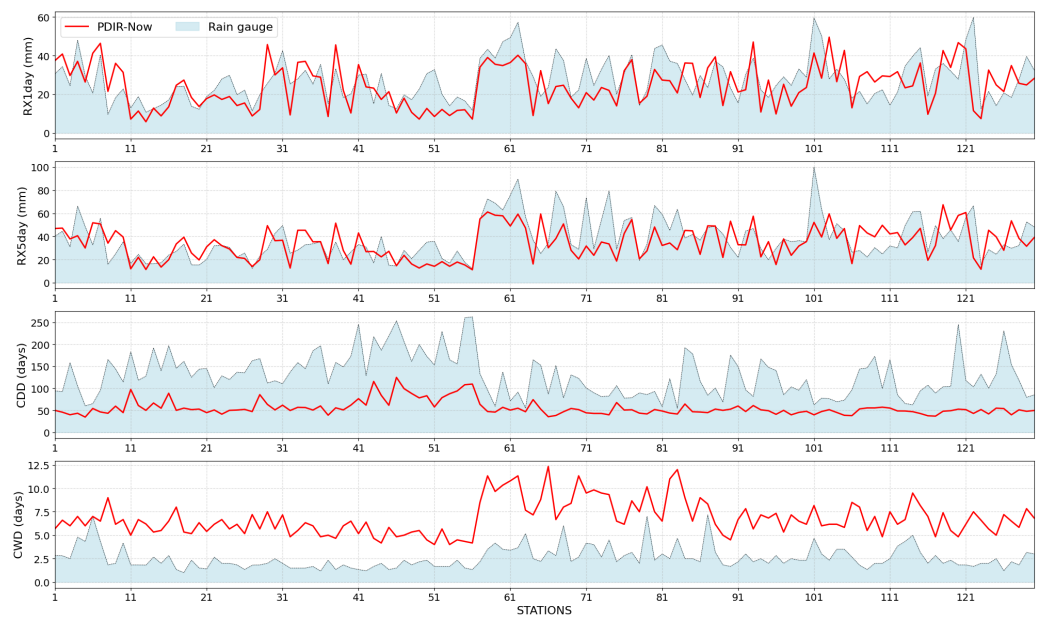


Figure 6. Extreme precipitation indices (RX1day, RX5day, CDD, and CWD) of PDIR-Now and rain gauge data at observed gauge stations.

In regards to the final two indices, PDIR-Now exhibits an underestimation of the CDD and an overestimation of CWD. This indicates that PDIR-Now captures longer wet spells and shorter dry spells than the rainfall gauges do. Figure 7 supports this by showing a large negative bias in the CDD, -74.25 days, and a positive mean bias in the CWD of 4.22 days. The difference in the values of the bias in the CDD and CWD corresponds to the fact that wet spells are usually a lot shorter than dry spells, especially in arid and semi-arid regions such as Saudi Arabia.

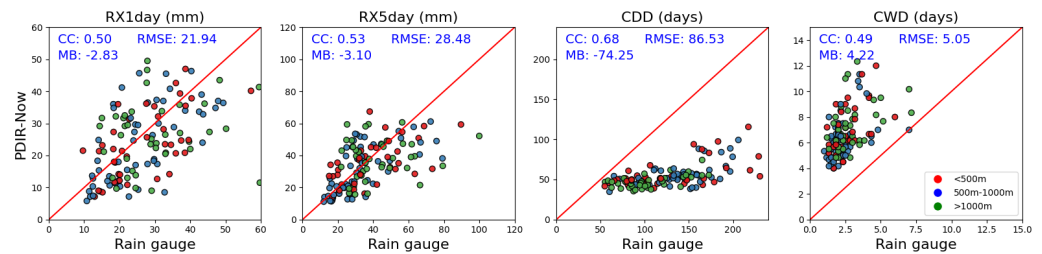


Figure 7. Scatter plots of PDIR-Now and rain gauge data for RX1day, RX5day, CDD, and CWD indices at different elevation thresholds with statistics of mean CC, MB, and RMSE.

Figure 8 illustrates the spatial pattern of extreme indices derived from both gauge data and PDIR-Now. The figure reveals that PDIR-Now demonstrates a similar spatial distribution in the RX1day and RX5day indices compared to the gauge data. However, the accurate representation of the spatial distribution of dry and wet spell durations is not achieved by PDIR-Now, as evident in the four rightmost panels of Figure 8. This observation aligns with expectations, given the superior performance demonstrated by PDIR-Now in the RX1day and RX5day indices, as depicted in Figure 6.

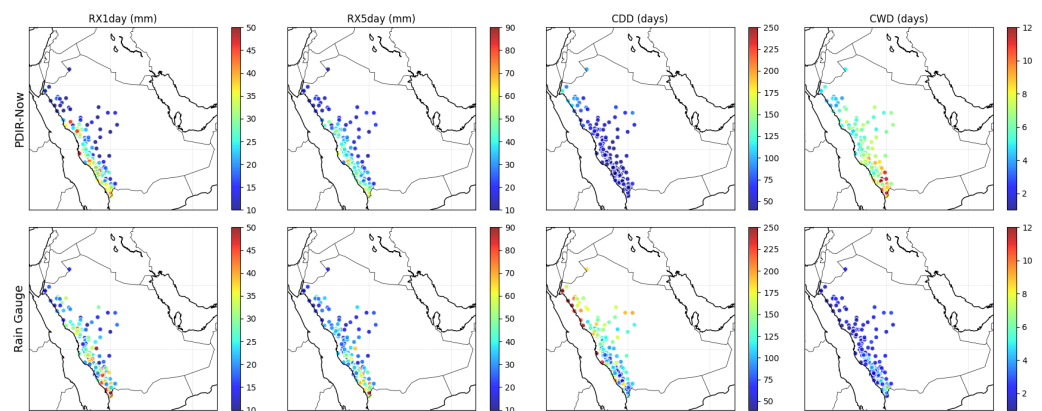


Figure 8. Spatial distribution of extreme precipitation indices (RX1day, RX5day, CDD, and CWD) of PDIR-Now and rain gauge data at observed gauge stations.

In addition, 130 rain gauge stations were classified into different altitude ranges: <500 m, 500 – 1000 m, and >1000 m. This categorization is employed to assess the performance of PDIR-Now across RX1day, RX5day, CWD, and CDD indices, considering various topographies. Stations below 500 m are represented by the color red, those between 500 m and 1000 m by blue, and those above 1000 m by green in Figure 7. A comprehensive statistical evaluation of PDIR-Now in comparison to the rain gauge data for RX1day, RX5day, CDD, and CWD indices across various topographies is presented in Table 4. The higher CC and lower RMSE and MB observed for stations with elevations <500 m and between 500 m to 1000 m confirm that PDIR-Now exhibits greater accuracy at elevations below 1000 m. As the altitude increases and the orographic effect of the southwestern mountain range comes into play, PDIR-Now exhibits poor performance above 1000 m, with a low CC of 0.18 for RX1day and 0.17 for RX5day, along with higher RMSE and MB compared to the stations below 1000 m.

Table 4. Performance of PDIR-Now compared to the rain gauge for RX1day, RX5day, CDD, and CWD indices across different elevation thresholds.

	RX1day (mm)	RX5day (mm)	CDD (Days)	CWD (Days)
Elevation < 500 m				
CC	0.60	0.60	0.58	0.57
RMSE	20.05	28.76	85.91	5.08
MB	−2.89	−3.98	−75.53	4.30
500–1000 m				
CC	0.64	0.66	0.76	0.42
RMSE	21.56	25.51	98.97	4.86
MB	−2.23	−1.62	−84.72	4.05
>1000 m				
CC	0.18	0.17	0.53	0.42
RMSE	24.31	32.23	70.24	5.28
MB	−3.58	−4.24	−60.73	4.38

4. Discussion

In this study, an evaluation of PDIR-Now’s performance was conducted, specifically focusing on its comparison against ground-based rain gauges. This analysis is implemented in the context of various geographical regions across Saudi Arabia, allowing for insights into the national effectiveness of PDIR-Now.

There are noticeable patterns of overestimation and underestimation within PDIR-Now’s rainfall estimations, particularly in connection to various rainfall rate categories. These patterns highlight the challenges faced by satellite-based precipitation products when estimating precipitation across a wide range of rainfall rates. It is crucial to carefully examine the topographical and geological variations within the research area. Factors such as topography, altitude, orographic effects, localized wind patterns, and microclimatic differences significantly affect the accuracy of remote sensing-based precipitation estimation products [45–47]. The algorithms employed in satellite-based precipitation products not only add an extra layer of complexity but also demonstrate their sensitivity to climatic conditions and precipitation event features [46,48].

There are several factors that can affect the accuracy of satellite precipitation products when evaluated against gauge data, such as orographic precipitation, spatial and temporal matching, and algorithm characteristics. Orographic precipitation usually falls into the category of warm precipitation, given that orographic lift is not conducive to producing frozen hydrometeors [49]. Moreover, warm precipitation is described as rainfall that occurs when there are no frozen hydrometeors present and the cloud-top temperature is above 273 K. IR-based algorithms, such as PDIR-Now, use a cloud-top temperature threshold that is then related to precipitation rate. Thus, if the cloud-top temperature is higher than the threshold, the precipitation will be underestimated by the product. The results of this paper confirm the limitation of IR algorithms in areas where orographic precipitation is present, as the accuracy of PDIR-Now diminished in areas prone to this type of precipitation. In terms of geospatial and temporal matching, each PDIR-Now pixel of $0.04^\circ \times 0.04^\circ$ is aligned with the corresponding rain gauge data point based on their coordinates. This can cause differences between the products, because a point measurement is compared to an estimate of an area of approximately 16 km². Additionally, the daily PDIR-Now, aggregated from half-hourly estimates, is synchronized with the daily readings from the rain gauge [28]. Systematic and aggregation errors during these processes could also contribute to the divergence between PDIR-Now and the rain gauges.

Furthermore, the length and quality of the accessible data are important in determining efficiency indicators in this study. The study’s 6-year duration enables an evaluation of PDIR-Now’s ability to accurately represent rainfall intensities compared to rain gauge data. Nevertheless, it is important to acknowledge the limitations of the existing ground truth

dataset with an uneven distribution of rain gauges across the region. Given the limited availability of observation data, this research is fundamentally comparative over a 6-year study period and should not be considered a conclusive basis for assessing the overall performance of PDIR-Now. A more thorough evaluation using over two decades of rainfall data is recommended.

As mentioned in the introduction, the past studies have assessed other SPPs over the country. However, the results between those studies and this one are not comparable. In each of these studies, the assessed periods are different. In the case of this study, the period between 2017 through 2022 is being assessed, whereas in other studies, such as Helmi and Abdelhamed [34], the period from 2000 to 2012 was used. Furthermore, in Kheimi and Gutub [31], January 2003 through November 2010 was utilized. Furthermore, in the past literature, there has not been a study that only assesses near-real-time products, which is the only type of product that PDIR-Now could be objectively compared to, due to the difference in purpose of near-real-time products and climate data records. Mahmoud et al. [32] assessed IMERG Early, NASA's near-real-time product, but the length of the study period, October 2015 to April 2016, does not match this study's. Additionally, the rain gauge network is different. Thus, the results from this study cannot be objectively compared to past studies.

This application of PDIR-Now is a good starting point for the assessment of this SPP over the study area. However, there is still plenty of space for improvement, particularly in arid and semiarid regions. An appropriate technique for future developments is minimizing the existing biases in PDIR-Now. This may be accomplished by using topographical data, considering other climatic features, and applying machine learning techniques [46,50]. It is essential to assess the accuracy of satellite products, such as PDIR-Now, and detect any hidden biases through comprehensive evaluations across different spatial and temporal scales. More validation findings for remote sensing precipitation products will hold significance and offer benefits across a wide range of applications, including hydrology, agriculture, and water management.

5. Conclusions

This study was the first one of its kind to test the capabilities of the latest near-real-time satellite product by the CHRS, PDIR-Now, over Saudi Arabia. This analysis involved a thorough approach of matching gauge-station coordinates with satellite precipitation coordinates, which enabled the evaluation of the SPP. By evaluating PDIR-Now against the rain gauge data, the study aimed to discern the product's strengths and limitations. The evaluation can be separated into two sections. First, six well-established statistical metrics were employed to assess the accuracy of PDIR-Now to detect rainfall events and their precipitation amounts at a daily scale. The metrics utilized to assess the accuracy of PDIR-Now in capturing precipitation amounts were the CC, the MB, and the RMSE, whereas the metrics for assessing the correctness of the rainfall detection were the POD, FAR, and CSI. Moreover, four annual extreme precipitation indices were used to analyze the capability of PDIR-Now when capturing extreme precipitation events. The extreme precipitation indices included in the study were RX1day, RX5day, CDD, and CWD.

Accurate estimates of precipitation are extremely valuable in arid and semi-arid areas. All of the tools used to measure or estimate precipitation have advantages and disadvantages. Even though the fine spatial and temporal resolutions of satellite products are a great advantage, these products also have limitations. SPP evaluations are essential and have great implications in assessing the validity of SPPs over Saudi Arabia. This is because given that these products can provide information about the spatial distribution of precipitation, they are very often used in studies related to hydrology and climatology. Thus, assessing their reliability is crucial. Additionally, having accurate near-real-time estimates of precipitation over the study area, including spatial distribution information, is key for water budget studies, thus, directly affecting water resources management. Furthermore, having a product that accurately depicts extreme events is useful for post-

disaster assessment, enabling prompt response in mitigating the impacts of these heavy precipitation events.

This analysis provided a depiction of PDIR-Now's performance over Saudi Arabia. PDIR-Now showed the ability to capture precipitation with a low MB of 0.07 mm/day and a CC of 0.33. In the case of the detection of precipitation, PDIR-Now showed a better capability in the southwestern part of the study area. In the categories analysis, PDIR-Now performed best in the detection of "Heavy Rain". Even though PDIR-Now shows higher POD in the "Light Rain" category, the accuracy of the detection is the best in the "Heavy Rain" category, shown by a higher CSI and lower FAR. Furthermore, PDIR-Now slightly overestimates "Light Rain" but underestimates "Moderate Rain" and "Heavy Rain". The error in the different categories is more prone to occur in areas affected by orographic precipitation, specifically the southwest of the country. In this region, the ability of PDIR-Now to capture small-scale, orographically induced rainfall events diminished, highlighting the importance of spatial resolution and topographical considerations. Additionally, PDIR-Now similarly captured the RX1day and RX5day precipitation amounts throughout the gauge locations with only a slight underestimation. On the other hand, the CDD was underestimated compared to the rainfall gauges, and the CWD was overestimated. This reveals that PDIR-Now captures shorter dry spells and longer wet spells than the rain gauge network. Concerning different topographies, PDIR-Now shows greater accuracy at elevations below 1000m, indicated by higher CC and lower RMSE and MB. However, its performance declines above 1000m due to the orographic effect of the southwestern mountain range, leading to much lower CC values (0.18 for RX1day and 0.17 for RX5day) and increased RMSE and MB compared to stations at lower altitudes.

In conclusion, this manuscript provides insight on the ability of PDIR-Now to provide accurate near-real-time precipitation estimates. It underscores the complexities and challenges inherent to remote sensing-based precipitation products while highlighting their potential in diverse applications. The study's insights pave the way for ongoing research, seeking to harness the full potential of satellite-based precipitation estimation for improved hydrological and climatological studies, water resource management, and disaster preparedness over Saudi Arabia.

Author Contributions: R.S.A. conceptualized the study, performed the initial calculations, and wrote the first version of the manuscript. V.D. finalized the calculations, visualized all figures, and edited the manuscript. C.J.A. made revisions to the manuscript and edited the text. P.N. guided the collaboration and revised the finalized document.

Funding: This research was funded by Researchers Supporting Project number (RSP-2021/310) and (RSP2024R310), King Saud University, Riyadh, Saudi Arabia

Data Availability Statement: New data was not created through this work.

Acknowledgments: The authors would like to acknowledge the King Saud University, Riyadh, Saudi Arabia, for their support of this work. We extend our thanks to colleagues in the Department of Surface Water and Dams for providing essential daily precipitation data for our research. Our appreciation also goes to H.E. A. Alshaibani, the Deputy Minister for Water Affairs, for his support and encouragement.

Conflicts of Interest: The authors declare no conflicts of interest.

Abbreviations

The following abbreviations are used in this manuscript:

CC	Correlation coefficient
CDD	Consecutive dry days
CHIRPS	Climate Hazards Group InfraRed Precipitation with Station
CHRS	Center for Hydrometeorology and Remote Sensing
CMORPH	Climate Prediction Center Morphing Technique

CSI	Critical success index
CWD	Consecutive wet days
FAR	False alarm ratio
GSMaP-MVK	Global Satellite Mapping of Precipitation Microwave-IR Combined Product
IMERG	Integrated Multi-satellite Retrievals for Global Precipitation Measurement
MB	Mean bias
MEWA	Ministry of Environment, Water, and Agriculture
PERSIANN	Precipitation Estimation from Remotely Sensed Information using Artificial Neural Networks
PDIR-Now	PERSIANN-Dynamic Infrared near-real-time
PERSIANN-CCS	PERSIANN-Cloud Classification System
PERSIANN-CDR	PERSIANN-Climate Data Record
POD	Probability of detection
RMSE	Root-mean-squared error
SPP	Satellite precipitation product
Tb-R	Cloud-top brightness temperatures-rain rate
TRMM	Tropical Rainfall Measuring Mission
WRCP	World Climate Research Programme

References

- Azeez, O.; Elfeki, A.; Kamis, A.S.; Chaabani, A. Dam Break Analysis and Flood Disaster Simulation in Arid Urban Environment: The Um Al-Khair Dam Case Study, Jeddah, Saudi Arabia. *Nat. Hazards* **2020**, *100*, 995–1011. [\[CrossRef\]](#)
- Gao, Z.; Long, D.; Tang, G.; Zeng, C.; Huang, J.; Hong, Y. Assessing the Potential of Satellite-Based Precipitation Estimates for Flood Frequency Analysis in Ungauged or Poorly Gauged Tributaries of China's Yangtze River Basin. *J. Hydrol.* **2017**, *550*, 478–496. [\[CrossRef\]](#)
- Katipoğlu, O.M.; Sarıgöl, M. Prediction of Flood Routing Results in the Central Anatolian Region of Türkiye with Various Machine Learning Models. *Stoch. Environ. Res. Risk Assess* **2023**, *37*, 2205–2224. [\[CrossRef\]](#)
- Yeditha, P.K.; Kasi, V.; Rathinasamy, M.; Agarwal, A. Forecasting of Extreme Flood Events Using Different Satellite Precipitation Products and Wavelet-Based Machine Learning Methods. *Chaos Interdiscip. J. Nonlinear Sci.* **2020**, *30*, 063115. [\[CrossRef\]](#)
- Zhao, Q.; Liu, K.; Sun, T.; Yao, Y.; Li, Z. A novel regional drought monitoring method using GNSS-derived ZTD and precipitation. *Remote Sens. Environ.* **2023**, *297*, 113778. [\[CrossRef\]](#)
- Katiraie-Boroujerdy, P.-S.; Nasrollahi, N.; Hsu, K.; Sorooshian, S. Evaluation of Satellite-Based Precipitation Estimation over Iran. *J. Arid. Environ.* **2013**, *97*, 205–219. [\[CrossRef\]](#)
- Nashwan, M.S.; Shahid, S.; Wang, X. Assessment of Satellite-Based Precipitation Measurement Products over the Hot Desert Climate of Egypt. *Remote Sens.* **2019**, *11*, 555. [\[CrossRef\]](#)
- Qin, Y.; Chen, Z.; Shen, Y.; Zhang, S.; Shi, R. Evaluation of Satellite Rainfall Estimates over the Chinese Mainland. *Remote Sens.* **2014**, *6*, 11649–11672. [\[CrossRef\]](#)
- Hong, Y.; Gochis, D.; Cheng, J.; Hsu, K.; Sorooshian, S. Evaluation of PERSIANN-CCS Rainfall Measurement Using the NAME Event Rain Gauge Network. *J. Hydrometeorol.* **2007**, *8*, 469–482. [\[CrossRef\]](#)
- Miao, C.; Ashouri, H.; Hsu, K.-L.; Sorooshian, S.; Duan, Q. Evaluation of the PERSIANN-CDR Daily Rainfall Estimates in Capturing the Behavior of Extreme Precipitation Events over China. *J. Hydrometeorol.* **2015**, *16*, 1387–1396. [\[CrossRef\]](#)
- Eini, M.R.; Rahmati, A.; Piniewski, M. Hydrological Application and Accuracy Evaluation of PERSIANN Satellite-Based Precipitation Estimates over a Humid Continental Climate Catchment. *J. Hydrol. Reg. Stud.* **2022**, *41*, 101109. [\[CrossRef\]](#)
- Najmi, A.; Igmoullan, B.; Namous, M.; El Bouazzaoui, I.; Brahim, Y.A.; El Khalki, E.M.; Saidi, M.E.M. Evaluation of PERSIANN-CCS-CDR, ERA5, and SM2RAIN-ASCAT Rainfall Products for Rainfall and Drought Assessment in a Semi-Arid Watershed, Morocco. *J. Water Clim. Chang.* **2023**, *14*, 1569–1584. [\[CrossRef\]](#)
- Rahmati Ziveh, A.; Bakhtar, A.; Shayeghi, A.; Kalantari, Z.; Bavani, A.M.; Ghajarnia, N. Spatio-Temporal Performance Evaluation of 14 Global Precipitation Estimation Products across River Basins in Southwest Iran. *J. Hydrol. Reg. Stud.* **2022**, *44*, 101269. [\[CrossRef\]](#)
- Arsenault, R.; Brissette, F. Determining the Optimal Spatial Distribution of Weather Station Networks for Hydrological Modeling Purposes Using RCM Datasets: An Experimental Approach. *J. Hydrometeorol.* **2014**, *15*, 517–526. [\[CrossRef\]](#)
- Guo, R.; Liu, Y. Evaluation of Satellite Precipitation Products with Rain Gauge Data at Different Scales: Implications for Hydrological Applications. *Water* **2016**, *8*, 281. [\[CrossRef\]](#)
- Kummerow, C.; Barnes, W.; Kozu, T.; Shiue, J.; Simpson, J. The Tropical Rainfall Measuring Mission (TRMM) Sensor Package. *J. Atmos. Oceanic Technol.* **1998**, *15*, 809–817. [\[CrossRef\]](#)
- Joyce, R.J.; Janowiak, J.E.; Arkin, P.A.; Xie, P. CMORPH: A Method That Produces Global Precipitation Estimates from Passive Microwave and Infrared Data at High Spatial and Temporal Resolution. *J. Hydrometeorol.* **2004**, *5*, 487–503. [\[CrossRef\]](#)
- Funk, C.; Peterson, P.; Landsfeld, M.; Pedreros, D.; Verdin, J.; Rowland, J.; Romero, B.E.; Husak, G.; Michaelsen, J.; Verdin, A. A Quasi-Global Precipitation Time Series for Drought Monitoring. *USGS Sci. Chang. World* **2014**, *832*, 4. [\[CrossRef\]](#)

19. Hsu, K.; Gao, X.; Sorooshian, S.; Gupta, H.V. Precipitation Estimation from Remotely Sensed Information Using Artificial Neural Networks. *J. Appl. Meteor.* **1997**, *36*, 1176–1190. [[CrossRef](#)]
20. Hong, Y.; Hsu, K.-L.; Sorooshian, S.; Gao, X. Precipitation Estimation from Remotely Sensed Imagery Using an Artificial Neural Network Cloud Classification System. *J. Appl. Meteorol.* **2004**, *43*, 1834–1853. [[CrossRef](#)]
21. Ashouri, H.; Hsu, K.-L.; Sorooshian, S.; Braithwaite, D.K.; Knapp, K.R.; Cecil, L.D.; Nelson, B.R.; Prat, O.P. PERSIANN-CDR: Daily Precipitation Climate Data Record from Multisatellite Observations for Hydrological and Climate Studies. *Bull. Am. Meteorol. Soc.* **2015**, *96*, 69–83. [[CrossRef](#)]
22. Eini, M.R.; Olyaei, M.A.; Kamyab, T.; Teymoori, J.; Brocca, L.; Piniewski, M. Evaluating Three Non-Gauge-Corrected Satellite Precipitation Estimates by a Regional Gauge Interpolated Dataset over Iran. *J. Hydrol. Reg. Stud.* **2021**, *38*, 100942. [[CrossRef](#)]
23. AghaKouchak, A.; Mehran, A.; Norouzi, H.; Behrangi, A. Systematic and Random Error Components in Satellite Precipitation Data Sets. *Geophys. Res. Lett.* **2012**, *39*, 2012GL051592. [[CrossRef](#)]
24. Sorooshian, S.; Hsu, K.-L.; Gao, X.; Gupta, V.; Imam, B.; Braithwaite, D. Evaluation of PERSIANN system satellite-based estimates of tropical rainfall. *Bull. Amer. Meteor. Soc.* **2000**, *81*, 2035–2046. [[CrossRef](#)]
25. Sun, Q.; Miao, C.; Duan, Q.; Ashouri, H.; Sorooshian, S.; Hsu, K. A Review of Global Precipitation Data Sets: Data Sources, Estimation, and Intercomparisons. *Rev. Geophys.* **2018**, *56*, 79–107. [[CrossRef](#)]
26. Zhou, L.; Koike, T.; Takeuchi, K.; Rasmy, M.; Onuma, K.; Ito, H.; Selvarajah, H.; Liu, L.; Li, X.; Ao, T. A Study on Availability of Ground Observations and Its Impacts on Bias Correction of Satellite Precipitation Products and Hydrologic Simulation Efficiency. *J. Hydrol.* **2022**, *610*, 127595. [[CrossRef](#)]
27. Al-Ahmadi, K.; Al-Ahmadi, S. Spatiotemporal variations in rainfall–topographic relationships in southwestern Saudi Arabia. *Arab J. Geosci.* **2014**, *7*, 3309–3324. [[CrossRef](#)]
28. Nguyen, P.; Ombadi, M.; Goroooh, V.A.; Shearer, E.J.; Sadeghi, M.; Sorooshian, S.; Hsu, K.; Bolvin, D.; Ralph, M.F. PERSIANN Dynamic Infrared–Rain Rate (PDIR-Now): A Near-Real-Time, Quasi-Global Satellite Precipitation Dataset. *J. Hydrometeorol.* **2020**, *21*, 2893–2906. [[CrossRef](#)]
29. Salehi, H.; Sadeghi, M.; Golian, S.; Nguyen, P.; Murphy, C.; Sorooshian, S. The Application of PERSIANN Family Datasets for Hydrological Modeling. *Remote Sens.* **2022**, *14*, 3675. [[CrossRef](#)]
30. Yaswanth, P.; Kannan, B.A.M.; Bindhu, V.M.; Balaji, C.; Narasimhan, B. Evaluation of Remote Sensing Rainfall Products, Bias Correction and Temporal Disaggregation Approaches, for Improved Accuracy in Hydrologic Simulations. *Water Resour. Manag.* **2023**, *37*, 3069–3092. [[CrossRef](#)]
31. Kheimi, M.M.; Gutub, S. Assessment of Remotely-Sensed Precipitation Products Across the Saudi Arabia Region. *Int. J. Water Resour. Arid. Environ.* **2015**, *4*, 76–88.
32. Mahmoud, M.T.; Al-Zahrani, M.A.; Sharif, H.O. Assessment of Global Precipitation Measurement Satellite Products over Saudi Arabia. *J. Hydrol.* **2018**, *559*, 1–12. [[CrossRef](#)]
33. Sultana, R.; Nasrollahi, N. Evaluation of Remote Sensing Precipitation Estimates over Saudi Arabia. *J. Arid. Environ.* **2018**, *151*, 90–103. [[CrossRef](#)]
34. Helmi, A.M.; Abdelhamed, M.S. Evaluation of CMORPH, Persiann-CDR, CHIRPS v2.0, TMPA 3b42 V7, and GPM IMERG V6 satellite precipitation datasets in Arabian arid regions. *Water* **2022**, *15*, 92. [[CrossRef](#)]
35. Almazroui, M. Temperature Variability over Saudi Arabia and Its Association with Global Climate Indices. *JKAU Met. Environ. Arid. Land Agric. Sci.* **2011**, *23*, 85–108. [[CrossRef](#)]
36. Almazroui, M. Sensitivity of a Regional Climate Model on the Simulation of High Intensity Rainfall Events over the Arabian Peninsula and around Jeddah (Saudi Arabia). *Theor. Appl. Climatol.* **2011**, *104*, 261–276. [[CrossRef](#)]
37. Almazroui, M. Rainfall Trends and Extremes in Saudi Arabia in Recent Decades. *Atmosphere* **2020**, *11*, 964. [[CrossRef](#)]
38. Al-Taher, A.A. Drought and Human Adjustment in Saudi Arabia. *GeoJournal* **1994**, *33*, 411–422. [[CrossRef](#)]
39. Al-Ahmadi, K.; Al-Ahmadi, S. Rainfall-Altitude Relationship in Saudi Arabia. *Adv. Meteorol.* **2013**, *2013*, 363029. [[CrossRef](#)]
40. Hasanean, H.; Almazroui, M. Rainfall: Features and Variations over Saudi Arabia, A Review. *Climate* **2015**, *3*, 578–626. [[CrossRef](#)]
41. Chen, C.; Li, Z.; Song, Y.; Duan, Z.; Mo, K.; Wang, Z.; Chen, Q. Performance of Multiple Satellite Precipitation Estimates over a Typical Arid Mountainous Area of China: Spatiotemporal Patterns and Extremes. *J. Hydrometeorol.* **2020**, *21*, 533–550. [[CrossRef](#)]
42. Katiraie-Boroujerdy, P.-S.; Ashouri, H.; Hsu, K.; Sorooshian, S. Trends of Precipitation Extreme Indices over a Subtropical Semi-Arid Area Using PERSIANN-CDR. *Theor. Appl. Climatol.* **2017**, *130*, 249–260. [[CrossRef](#)]
43. Liu, J.; Xia, J.; She, D.; Li, L.; Wang, Q.; Zou, L. Evaluation of Six Satellite-Based Precipitation Products and Their Ability for Capturing Characteristics of Extreme Precipitation Events over a Climate Transition Area in China. *Remote Sens.* **2019**, *11*, 1477. [[CrossRef](#)]
44. Rojas, Y.; Minder, J.R.; Campbell, L.S.; Massmann, A.; Garreaud, R. Assessment of GPM IMERG satellite precipitation estimation and its dependence on microphysical rain regimes over the mountains of south-central Chile. *Atmos. Res.* **2021**, *253*, 105454. [[CrossRef](#)]
45. Barros, A.P.; Kuligowski, R.J. Orographic Effects during a Severe Wintertime Rainstorm in the Appalachian Mountains. *Mon. Wea. Rev.* **1998**, *126*, 2648–2672. [[CrossRef](#)]
46. Chen, H.; Sun, L.; Cifelli, R.; Xie, P. Deep Learning for Bias Correction of Satellite Retrievals of Orographic Precipitation. *IEEE Trans. Geosci. Remote Sens.* **2022**, *60*, 4104611. [[CrossRef](#)]

47. Zhao, Q.; Wang, W.; Li, Z.; Du, Z.; Yang, P.; Yao, W.; Yao, Y. A high-precision ZTD interpolation method considering large area and height differences. *GPS Solut.* **2024**, *4*, 28. [[CrossRef](#)]
48. Derin, Y.; Anagnostou, E.; Berne, A.; Borga, M.; Boudevillain, B.; Buytaert, W.; Chang, C.-H.; Chen, H.; Delrieu, G.; Hsu, Y.; et al. Evaluation of GPM-Era Global Satellite Precipitation Products over Multiple Complex Terrain Regions. *Remote Sens.* **2019**, *11*, 2936. [[CrossRef](#)]
49. Hobouchian, M.P.; Salio, P.; García Skabar, Y.; Vila, D.; Garreaud, R. Assessment of satellite precipitation estimates over the slopes of the subtropical Andes. *Atmos. Res.* **2017**, *190*, 43–54. [[CrossRef](#)]
50. Tao, Y.; Gao, X.; Hsu, K.; Sorooshian, S.; Ihler, A. A Deep Neural Network Modeling Framework to Reduce Bias in Satellite Precipitation Products. *J. Hydrometeorol.* **2016**, *17*, 931–945. [[CrossRef](#)]

Disclaimer/Publisher’s Note: The statements, opinions and data contained in all publications are solely those of the individual author(s) and contributor(s) and not of MDPI and/or the editor(s). MDPI and/or the editor(s) disclaim responsibility for any injury to people or property resulting from any ideas, methods, instructions or products referred to in the content.